Journal of Applied Polymer Science

Flame-retardant and thermal degradation mechanism of low-density polyethylene modified with aluminum hypophosphite and microencapsulated red phosphorus

De Kang Wang, Hui He, Peng Yu
College of Materials Science and Engineering, South China University of Technology, Guangzhou 510640, China
Correspondence to: H. He (E-mail: pshuihe@scut.edu.cn)

ABSTRACT: Aluminum hypophosphite (AHP), a novel flame retardant, was used to improve the flame retardancy of low-density polyethylene (LDPE) with microencapsulated red phosphorus (MRP). The synergistic effect between MRP and AHP was investigated by the limiting oxygen index (LOI), vertical burning test (UL-94), and thermogravimetric analysis. When the contents of MRP and AHP were 10 and 30 phr, the LOI of LDPE/10MRP/30AHP composite was 25.5%, and it passed the UL-94 V-0 rating (the number before "MRP" and "AHP" is the loading of MRP and AHP, In LDPE/10MRP/30AHP, the content of the LDPE, MRP and AHP is 100phr, 10phr and 30phr, where phr refers to parts per hundreds of resin). The results of cone calorimetry testing show that the heat release rate of the composites was significantly reduced, and the strength of the char layer improved when the loading of AHP increased. The thermal stability of the LDPE/10MRP/30AHP composite was enhanced. The structure of the char was investigated by Fourier transform infrared spectrometry and scanning electron microscopy/energy-dispersive spectrometry. The results indicate that AHP promoted the formation of stable char. This research provided a good way to prepare flame-retardant materials with a halogen-free flame retardant and contributed to environmental protection. © 2015 Wiley Periodicals, Inc. J. Appl. Polym. Sci. **2016**, *133*, 43225.

KEYWORDS: flame retardance; functionalization of polymers; polyolefins

Received 19 August 2015; accepted 14 November 2015
DOI: 10.1002/app.43225

INTRODUCTION

Low-density polyethylene (LDPE) is used widely in many fields because of its advanced mechanical properties and excellent processing performance. However, because of the poor flame retardancy of LDPE, its applications are limited in some areas where excellent flame retardancy is required. To improve LDPE's flame retardancy, researchers have conducted comprehensive investigations to study and develop novel flame-retardant additives.

Halogen-containing compounds have excellent fire resistance for LDPE, but this kind of flame retardant produces some toxic gases when burned and may endanger people's lives and property safety.[1] Now, many countries prohibit the use of halogen-containing compounds. As a result, the development of halogen-free flame retardants has gained more attention.

Intumescent flame retardants (IFRs) have been widely used in polyolefin.[2] Typically, IFRs include three components: an acid source, a carbonization agent, and a blowing agent. These kinds of flame retardants are very effective because of their typical condensed-phase activity. However, IFR additives also have some disadvantages, such as a high loading and cost and a loss of the mechanical properties.

Furthermore, many kinds of inorganic materials are applied to obtain flame retardancy in LDPE. Metallic hydroxides,[3–6] such as magnesium hydroxide and aluminum hydroxide, can decompose exothermally with the release of water. The accompanying water vapor dilutes the flammable gas, and the decomposition products also insulate the polymer matrix from the heat source. However, they must be used in large amounts, and this leads to a loss in the mechanical properties of the composites. Clay[7] can contribute to the formation of protective barrier layers because layered silicates act in the condensed phase and behave like inert fillers. A small amount of layered double hydroxide (LDH) can improve the thermal stability and decrease the heat release rate (HRR) of the composite.[8,9] However, it is difficult to achieve a UL-94 rating with LDPE with only clay or LDH.

Aluminum hypophosphite (AHP) is a kind of novel inorganic flame retardant; it has attracted a large amount of attention because of its high efficiency in flame retardance.[10–15] However, it is rarely used in polyolefin. Microencapsulated red phosphorus (MRP) is type of efficient flame retardant used in many

Table I. Data before and after Microencapsulation for RP

Sample	Antioxidant [mg (g h)$^{-1}$]	PH_3 released [μg (g 24 h)$^{-1}$]	Ignition point (°C)	Water absorption for 15 days (%)
RP	50	27.9	453	33.3
MRP	15.2	4.1	466	5.6

polymers. A small amount of MRP combined with another flame retardant, such as aluminum hydroxide,[16] magnesium hydroxide,[17] or kaolin,[18] improves the flame retardancy of polymers significantly. In addition, to the best of our knowledge, there are have been reports on AHP and MRP in LDPE. The aim of this research was to combine the flame retardant AHP with MRP to significantly improve the flame retardancy of LDPE. The flammability and thermal degradation behavior of LDPE/10MRP/30AHP composites were studied, and the synergistic effect between MRP and AHP was also investigated (the number before "MRP" and "AHP" is the loading of MRP and AHP, In LDPE/10MRP/30AHP, the content of the LDPE, MRP and AHP is 100phr, 10phr and 30phr, where phr refers to parts per hundreds of resin).

EXPERIMENTAL

Materials

In this study, LDPE (19E) was obtained from China National Petroleum Corp. AHP (98%) was supplied by Qingyuan City Yicheng Flame-Retardant Materials Co., Ltd. (China). MRP was prepared in our laboratory.

Measurements

Fourier transform infrared (FTIR) spectra were recorded by a MAGNA-IR 760 spectrometer (Nicolet) with a KBr disk. The wave number was set in the range 4000–400 cm^{-1}.

The surface morphology of the char residue after the limiting oxygen index (LOI) test was observed with a scanning electron microscope (EVO 18, Zeiss, Germany). X-ray energy-dispersive spectroscopy (EDS) results were obtained.

The LOI test was performed with an oxygen index instrument (FTT, England) according to ASTM D 2863-2008. The dimensions of the tested samples were 80 × 10 × 4 mm^3.

The vertical burning (UL-94) test was conducted on a vertical burning instrument (FTT, England) according to ASTM D 635. The dimensions of the tested samples were 130 × 13 × 4 mm^3.

The combustion behaviors were measured with a cone calorimeter device (Fire Testing Technology). Samples with dimensions of 100 × 100 × 4 mm^3 were exposed to a radiant cone at a heat flux of 35 kW/m^2.

Thermogravimetric analysis (TGA) was carried out on a TG 209F1 (Netzsch, Germany), and the temperature range was 30–700°C at a heating rate of 20°C/min under N_2, and the flow rate was 15 mL/min.

Tensile tests were conducted on an electromechanical universal testing machine (Zwick Roell Z010, Germany) according to GB/T 1040–2006. The testing speed for tensile strength testing was 50 mm/min; the flexural tests were conducted on the same machine according to GB/T 9341-2008.

Capillary rheological properties was tested on a capillary rheometer (CFT-500D, Shimadzu, Japan) with different loads at 170°C.

Preparation of MRP

To improve the stability of red phosphorus (RP), MRP was prepared according to previous literature.[19,20] Some RP was added to an alcohol-soluble phenolic resin that was prepared in our laboratory; then, the mixture was stirred for 4 h. After that, the ethanol was evaporated at 80°C, and the solid was ground. The resulting powder was PF–RP.

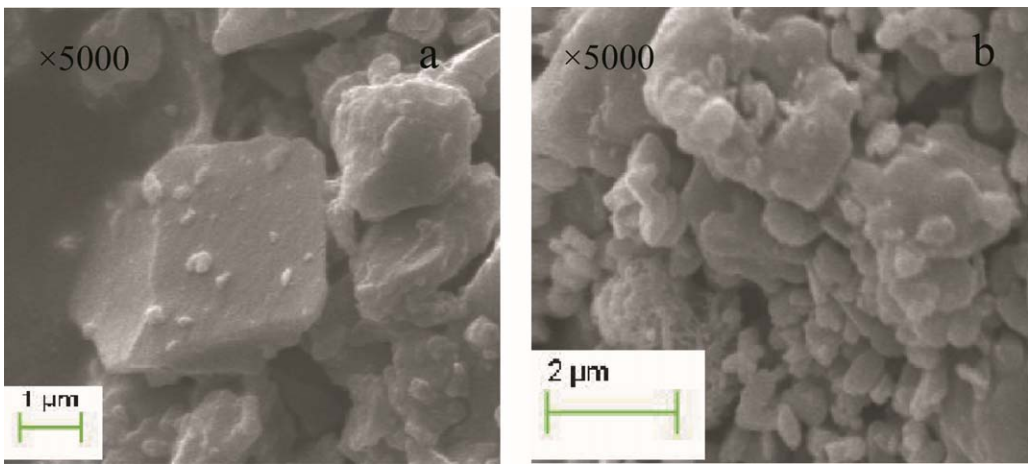

Figure 1. SEM photographs of (a) RP and (b) MRP. [Color figure can be viewed in the online issue, which is available at wileyonlinelibrary.com.]

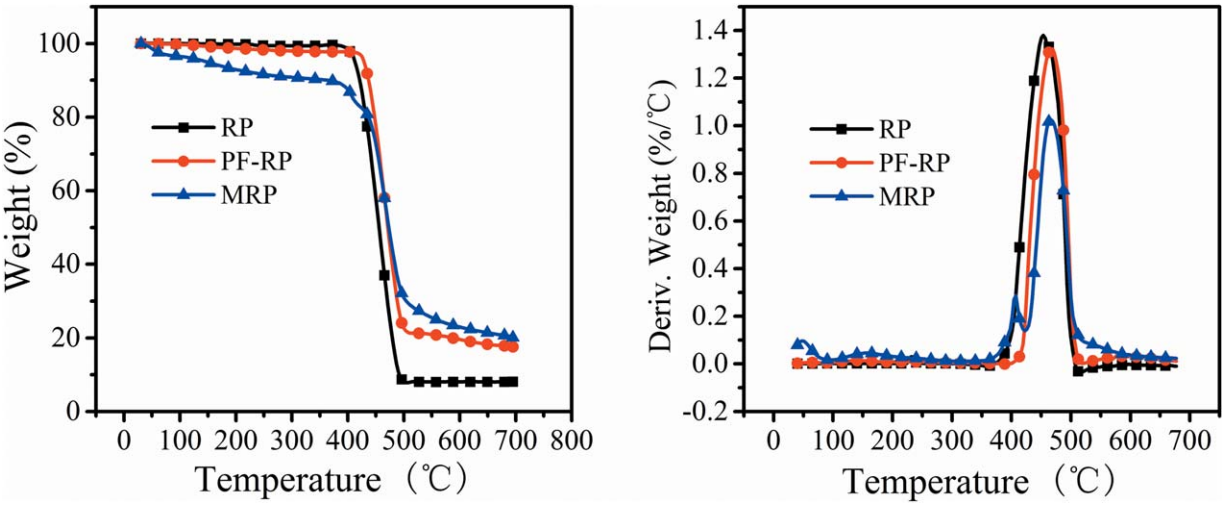

Figure 2. (a) TGA and (b) DTG curves of RP, RP–PF, and MRP under N_2. [Color figure can be viewed in the online issue, which is available at wileyonlinelibrary.com.]

A calculated amount of fine PF–RP powder was predispersed in water with sodium dodecyl sulfate in a three-necked flask equipped with a stirrer. An aqueous solution of melamine resin prepolymer (ca. 10%) was added to conduct the reaction for 2 h at 80°C. When the reaction was over, the pH value of the solution was adjusted to 7 with sodium hydroxide. The solid was then filtered, and these powders were processed by coloring agents. Finally, the powder after the coloring process was again microencapsulated by melamine resin. The final product was MRP.

Preparation of the Samples

MRP and AHP were dried in a vacuum oven at 100°C for 4 h. LDPE samples with different ratios of MRP, AHP, and other additives were prepared in an open mill for 5 min at 120°C. Finally, the samples were formed at 150°C.

RESULTS AND DISCUSSION

Stability of MRP

RP can easily absorb and react with water when exposed to air;[21] the method of microencapsulation can significantly prevent this reaction and water absorption. The antioxidant, PH_3 released, ignition point, and water absorption of the premicroencapsulation and postmicroencapsulation for RP are listed in Table I.

Compared with RP, MRP showed apparent changes in antioxidant, PH_3 released, ignition point, and water absorption. The water absorption of RP was very high with a moisture absorption rate of 33.3% after 15 days. In contrast, the moisture absorption rate of MRP was 5.6%. In addition, the ignition of MRP was improved by 13°C compared to that of RP. RP could be oxidized, and this released PH_3 into the air. After microencapsulation, the antioxidant and PH_3 release decreased. These results indicate that a good barrier was built by the resin coating, and this effectively stopped RP from touching the air. In addition, in the scanning electron microscopy (SEM) photographs of MRP and RP shown in Figure 1, the encapsulated layer can be clearly seen. Consequently, the stability of RP was significantly enhanced after microencapsulation.

TGA was used to study the thermal stability of pre-RP-microencapsulation and post-RP-microencapsulation. Figure 2 shows the TGA and differential thermogravimetry (DTG) curves of RP, PF–RP, and MRP in an N_2 atmosphere, and the corresponding characteristic data are listed in Table II.

Table II. Data of TGA and DTG for Various Samples at a Heating Rate of 20°C/min in N_2

Sample	$T_{initial}$ (°C)	Residue at 700°C (wt %)	T_{max} (°C)	
			Stage 1	Stage 2
RP	412	10.17	—	453
PF-RP	427	17.5	—	466
MRP	137	20.17	406	466

Table III. LOI and UL-94 Test Results for LDPE with Different Contents of MRP and AHP

Composition (phr)			LOI (%)	UL-94		
LDPE	MRP	AHP		$t_1 + t_2$ (s)	Dripping	Rating
100	0	0	19	BC	Yes	NR
100	8	0	22.0	10.6	Yes	V-2
100	10	0	22.6	26.6	Yes	V-2
100	12	0	22.3	18.7	Yes	V-2
100	0	20	24.8	BC	Yes	NR
100	0	30	25.5	BC	Yes	NR
100	0	40	26.4	25.1	No	V-2
100	10	10	25.3	BC	Yes	NR
100	10	20	25.4	BC	Yes	NR
100	10	30	25.5	5.1	No	V-0
100	10	40	25.8	5.3	No	V-0

BC, burns to clamp; NR, no rating; t_1 and t_2, average combustion times after the first and second applications of the flame, respectively.

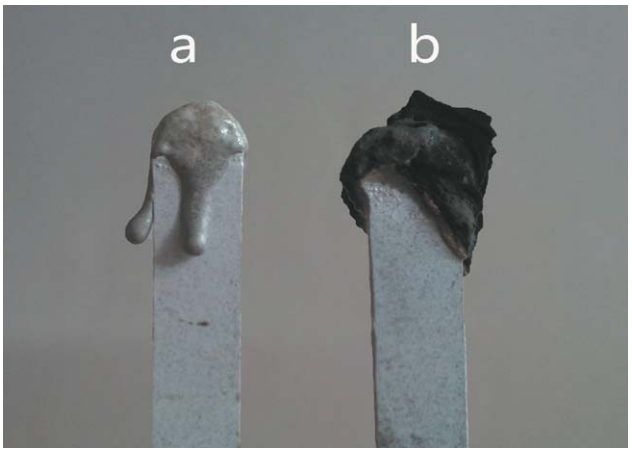

Figure 3. Digital photographs of the (a) LDPE/10MRP and (b) LDPE/10MRP/30AHP composites after the LOI tests. [Color figure can be viewed in the online issue, which is available at wileyonlinelibrary.com.]

RP started to degrade at 412°C, and only one severe decomposition process, located at about 453°C, was found. PF–RP had a similar thermal decomposition behavior to RP, but the temperature at which 5% weight loss occurred ($T_{initial}$) and the temperature at the maximum weight loss rate (T_{max}) increased to 427 and 466°C, respectively. Obviously, the thermal stability of RP was enhanced. This was mainly attributed to the formation of char by phenolic resin, which had a high char yield. For MRP, there were two main decomposition processes at about 406 and 466°C; the decomposition processes before 400°C may have been caused by the degradation of small molecules. The first decomposition process was attributed to the degradation of melamine resin, and the second was attributed to the degradation of RP. Despite the unchanged T_{max} of MRP compared with PF–RP, the maximum weight loss rate apparently decreased in the DTG curve; this indicated that the melamine resin coating slowed down the degradation of MRP. Meanwhile, the char residue increased with the addition of resin, and the formation of the carbon layer improved the stability of RP.

Flammability of the Composites

As shown in Table III, neat LDPE is a flammable plastic, and its LOI value is only about 19%. For LDPE/MRP composites, the LOI value ascended slowly with increasing MRP. When the loading was 10 phr, the LOI value of the LDPE/MRP composite was 22.6%. As for LDPE/AHP composites, the LOI value increased significantly with increasing content of AHP. The LOI value of the LDPE/AHP composite reached 26.4% when the AHP content was 40 phr; this was an increase of 38.9% compared with the value of neat LDPE. Therefore, both MRP and AHP were effective in improving the LOI value of LDPE. Figure 3 shows digital pictures after LOI testing of the LDPE/10MRP and LDPE/10MRP/30AHP composites. Clearly, the char residue of the LDPE/10MRP composite was very small. In contrast, the LDPE/10MRP/30AHP composite had much char residue. These results indicate that AHP played a key role in the process of char formation.

As shown in Table III, the neat LDPE showed no rating in the UL-94 test, and it had very serious dripping. With the addition

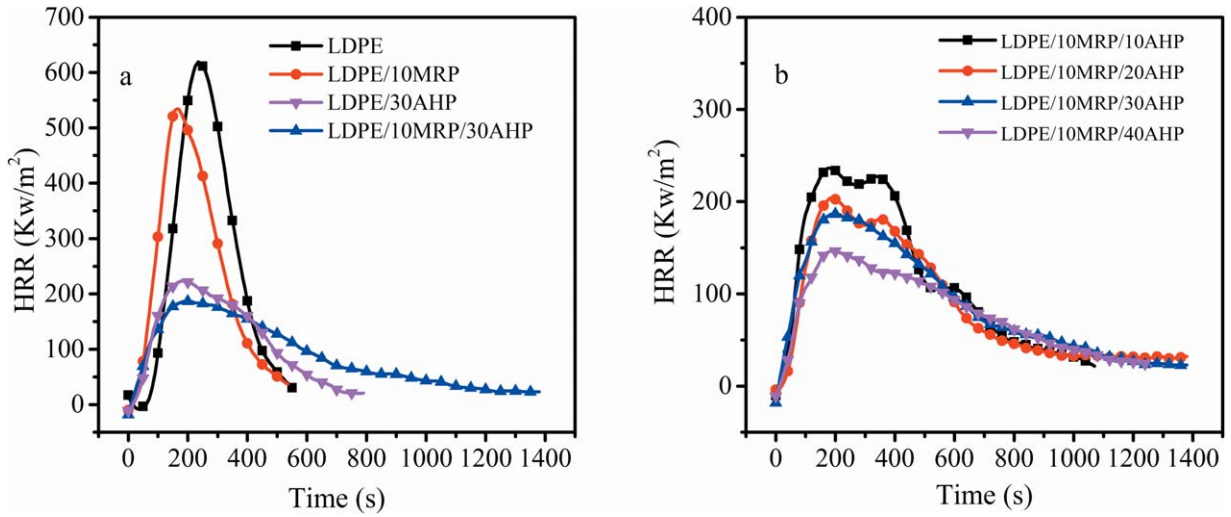

Figure 4. Cone calorimetry HRR curves for the composites. [Color figure can be viewed in the online issue, which is available at wileyonlinelibrary.com.]

Table IV. Cone Calorimetry Data for Composites (35 kW/m^2)

Sample	TTI (s)	T_p (s)	PHRR (kW/m^2)	THR (MJ/m^2)	MLR (g/s)	Residual char (%)
LDPE	67	240	636	139	0.06	3.5
LDPE/10MRP	33	160	550	126	0.0595	15.2
LDPE/30AHP	43	180	208	117	0.03	28.7
LDPE/10MRP/30AHP	34	190	189	120	0.02	31.3

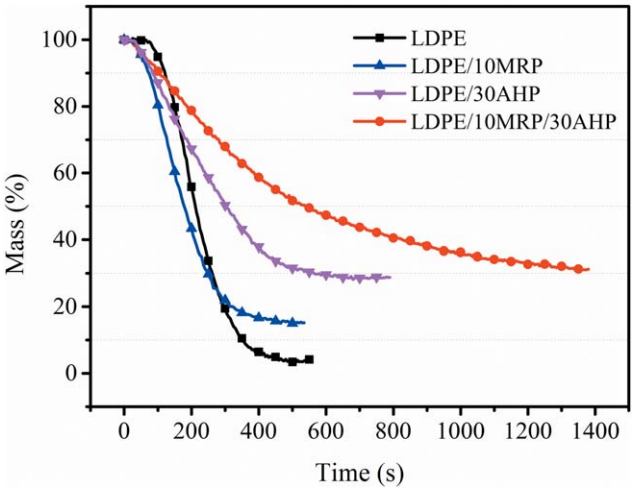

Figure 5. Mass loss plots of the neat LDPE and flame-retardant LDPE. [Color figure can be viewed in the online issue, which is available at wileyonlinelibrary.com.]

of MRP, the LDPE/MRP composite passed the UL-94 V-2 rating, and dripping still existed. The LDPE/AHP composite showed no rating in the UL-94 test and showed dripping as the content of AHP increased from 10 to 30 phr. When the content of AHP was 40 phr, the LDPE/AHP composite passed the UL-94 V-2 rating, and the dripping disappeared.

As for the LDPE/10MRP/AHP composite, when the content of AHP was 30 phr, the LDPE/10MRP/30AHP composite passed the UL-94 V-0 rating with no dripping, whereas the LDPE/10MRP and LDPE/30AHP composite had no rating at the same loading of correspondent flame retardant. This indicated that the flame-retardant efficiency was much higher when MRP and AHP were combined than when they were used singly. This may have been because of the synergistic effect of MRP and AHP. This synergistic effect is discussed later.

Cone calorimetry was used to investigate the influence of the flame-retardant content on the flammability of the composites. HRR is considered to be a powerful indicator in the evaluation

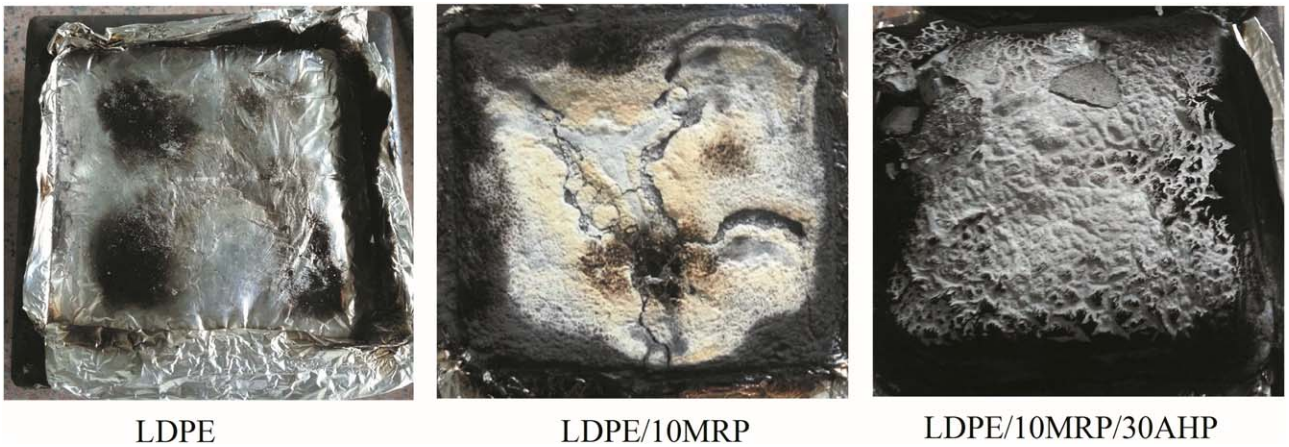

Figure 6. Digital pictures of the residue char after cone calorimetry testing. [Color figure can be viewed in the online issue, which is available at wileyonlinelibrary.com.]

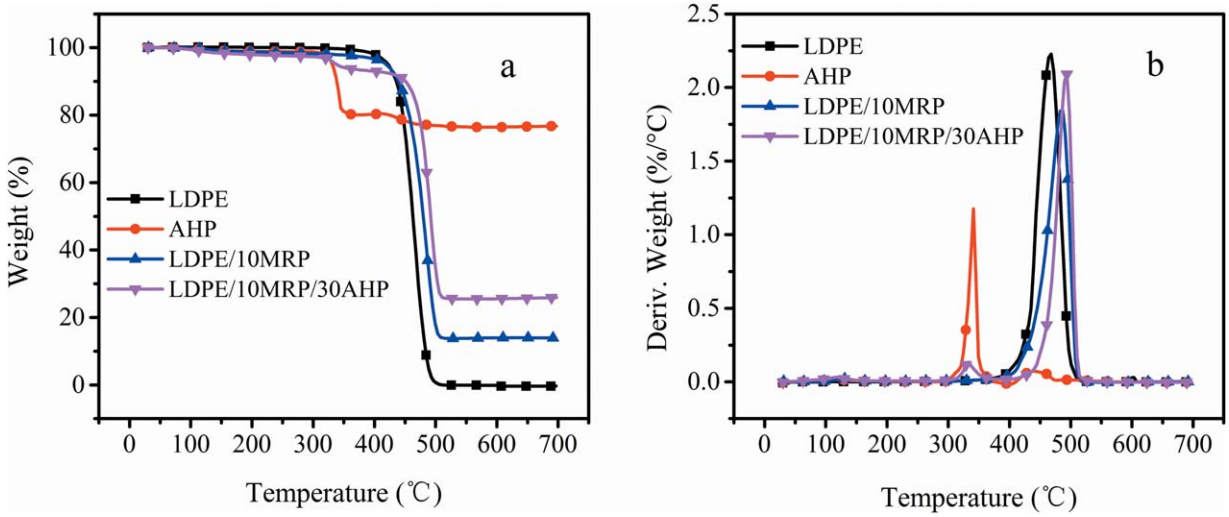

Figure 7. TGA and DTG curves of the pure LDPE, AHP, LDPE/10MRP, and LDPE/10MRP/30AHP. [Color figure can be viewed in the online issue, which is available at wileyonlinelibrary.com.]

Table V. Data for TGA and DTG for Various Samples at a Heating Rate of 20°C/min in N_2

Sample	$T_{initial}$ (°C)	Residue at 700°C (wt %)	T_{max} (°C)	
			Stage 1	Stage 2
LDPE	421	0	—	466
AHP	331	76.46	341	438
LDPE/10MRP	442	13.87	—	485
LDPE/10MRP/30AHP	336	25.49	331	492

of the fire hazardousness of materials, quantify fire size, and rate of fire growth. Figure 4 shows the HRR curve of the neat LDPE, LDPE/10MRP, and LDPE/10MRP/AHP composites with different loadings of AHP. The detailed cone calorimetric parameters of the neat LDPE and LDPE/10MRP/AHP composites at an incident heat flux of 35 kW/m^2 are listed in Table IV. The data include the time to ignition (TTI), peak heat release rate (PHRR), time to the peak heat release rate (T_p), total heat release (THR), mean mass loss rate (MLR), and value of the residual char.

Neat LDPE burned quickly after ignition and had a sharp peak, with a PHRR as high as 636 kW/m^2. LDPE/10MRP had a similar HRR curve as LDPE, and its HRR was still high. However, the HRR of LDPE/10MRP/30AHP composites decreased obviously, and the PHRR was 189 kW/m^2 at 190 s. The reduction of TTI might have been because of the initial combustion of flame retardants before these could play their role in the materials. Figure 5 shows the mass loss plot for the samples. MRP and AHP increased the burning residues of the LDPE/10MRP composites. In addition, when AHP and MRP were combined, the burn time of the composite was longer, and MLR was lower. These indicated that MRP and AHP had a good synergistic effect, and the composite exhibited more difficulty propagating flame than neat LDPE.

Figure 6 shows the digital pictures of the char residue of the neat LDPE, LDPE/MRP, and LDPE/10MRP/30AHP after the test. It was clear that LDPE/10MRP/30AHP formed a compact and stable char, whereas the neat LDPE left almost nothing, and the char of LDPE/10MRP was easily damaged. These results indicate that AHP promoted the formation of the char. In addition, as shown in Figure 3(b), two PHRRs appeared in the curve of the LDPE/10MRP/AHP composites with a low loading of AHP, whereas only one was found when the loading of AHP was high. This phenomenon was caused by the cracking char.[22] In other words, the char formed was more stable when the loading of AHP was 30 or 40 phr, and this stable char effectively slowed down heat and gas transference between the burning zone and the polymer matrix beneath. These results also are demonstrated in the SEM images.

Thermal Decomposition Behavior

The degradation behaviors of the neat LDPE, LDPE/10MRP/30AHP, LDPE/10MRP, and AHP were investigated by TGA under a nitrogen atmosphere. The TGA and DTG curves are presented in Figure 7, respectively, and the corresponding decomposition data are listed in Table V.

The neat LDPE started to degrade at 421°C and had only one stage to decompose; it did not leave any char residue at 700°C. The $T_{initial}$ of AHP was 331°C, and the maximum mass loss occurred at 341 and 438°C, respectively. When the addition of the MRP and AHP, two decomposition processes were found, and the $T_{initial}$ of the LDPE/10MRP/30AHP composite decreased to 336°C. This resulted from the degradation of AHP. However, T_{max2} increased from 466 to 492°C [where T_{max2} is the temperature at the second peak of DTG (derivative thermogravimetric analysis) curve]. This indicated the improved thermal stability of LDPE in the high-temperature area, and this degradation stage could have been related to the degradation of the LDPE matrix and the further degradation of AHP and MRP. Meanwhile, the LDPE/10MRP/30AHP composite possessed an obviously greater amount of char residue than LDPE at 700°C, and these results indicate a strong interaction between the flame retardant and the polymer. This led to the formation of more thermally stable residues. What is more, we observed that the char residue increased with increasing AHP, as shown in Table V. We demonstrated that AHP promoted char residue formation.

Combustion Residue

The FTIR spectra of the char residue of LDPE/10MRP and LDPE/10MRP/30AHP are shown in Figure 8. The broad absorbance at 3300–2850 cm^{-1} was attributed to the stretching vibrations of C—H. Moreover, the absorbance peak at 2850–3000 cm^{-1} was assigned to the stretching vibrations of saturated C—H; this indicated that LDPE did not decompose completely.[23] In addition, the absorbance peaks at 3000–3300 cm^{-1} were related to the stretching vibrations of unsaturated C—H. For LDPE/10MRP, C=O stretching vibrations at 1736 and

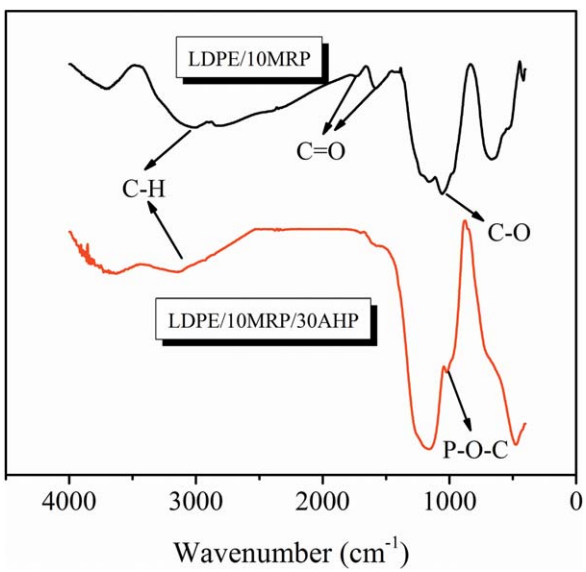

Figure 8. FTIR spectra of the char residues of the composite after LOI testing. [Color figure can be viewed in the online issue, which is available at wileyonlinelibrary.com.]

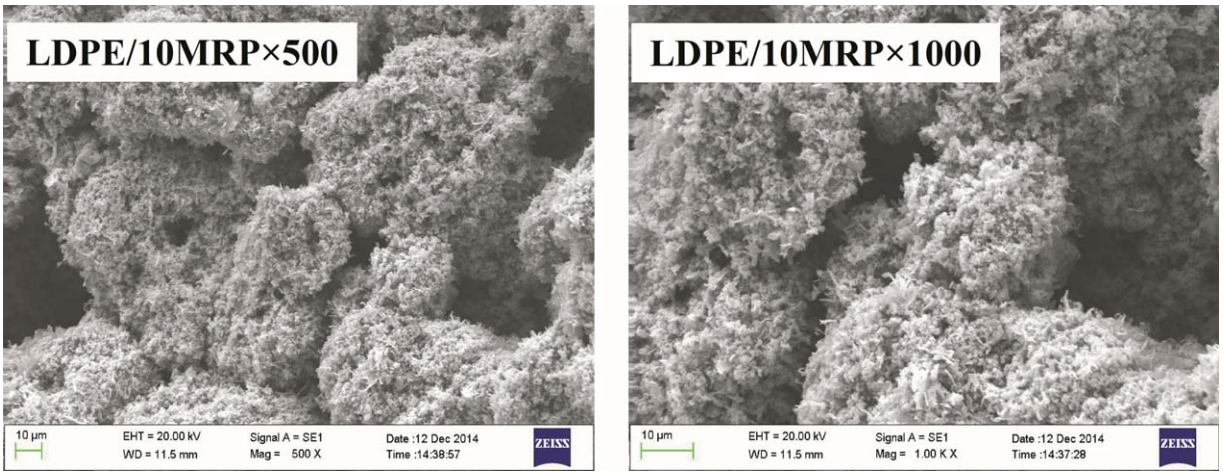

Figure 9. SEM images of the char residues of LDPE/10MRP. [Color figure can be viewed in the online issue, which is available at wileyonlinelibrary.com.]

1580 cm^{-1} were detected. The peak[23] at 1100–1200 cm^{-1} was attributed to PO_4^{3-}, and the C—O absorbance was mainly distributed at 1050 cm^{-1}. As to LDPE/10MRP/30AHP, the absorbance peaks between 1500 and 1800 cm^{-1} may have included the peaks at C═O bond (1650–1740 cm^{-1})[24] and C═C of the olefins (1675–1640 cm^{-1}) and polyaromatic carbons (1535 cm^{-1}). The peak at 1100 cm^{-1} was attributed to PO_4^{3-}, and the PO_2^- absorbance was mainly distributed at 1240 and 1024 cm^{-1}.[23] In addition, the peak observed at 1020 cm^{-1} was assigned to P—O—C; this indicated the formation of a new P—O—Φ structure,[25,26] where Φ is the obvious fragment of LDPE. Moreover, the peak at 480 cm^{-1} was assigned to Al—O.[27]

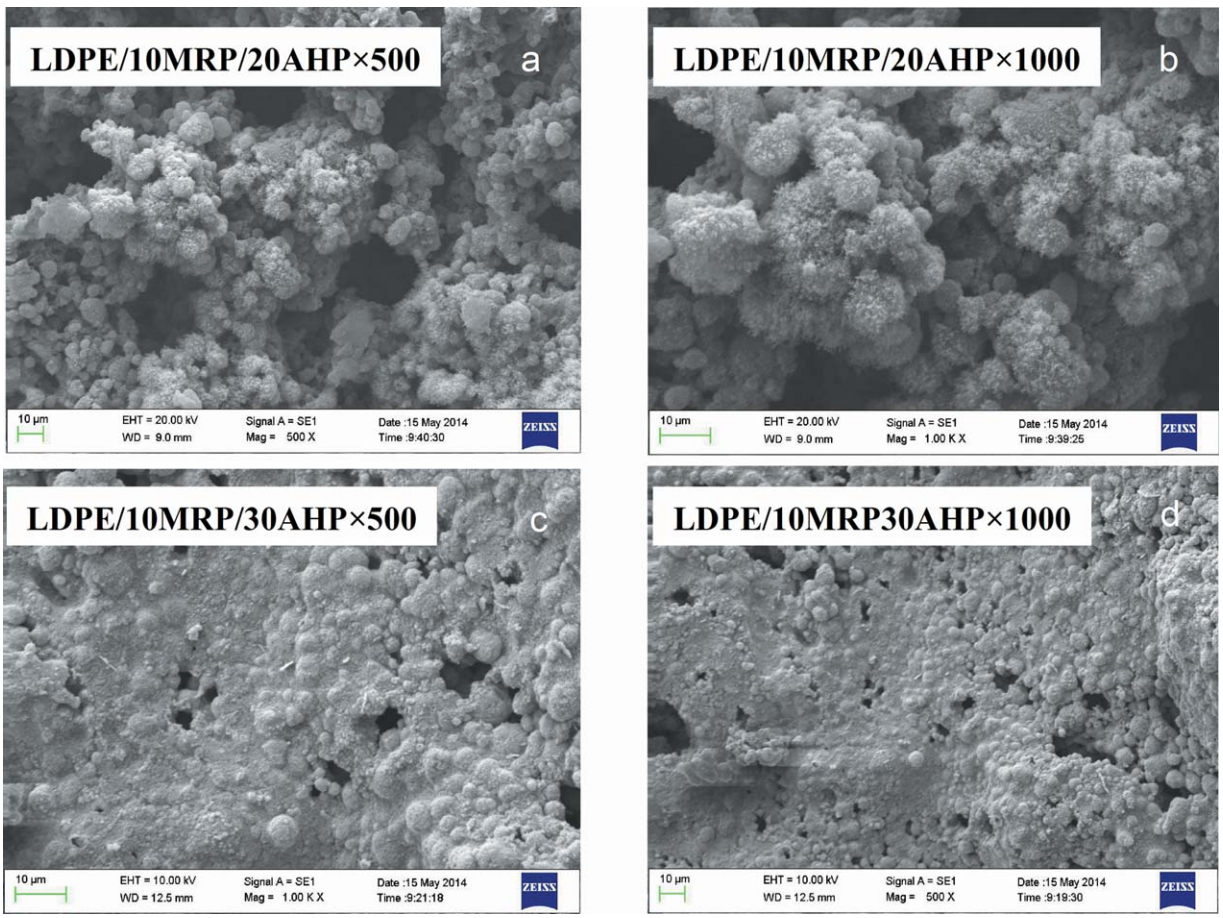

Figure 10. SEM images of the char residues for the composites after LOI testing. [Color figure can be viewed in the online issue, which is available at wileyonlinelibrary.com.]

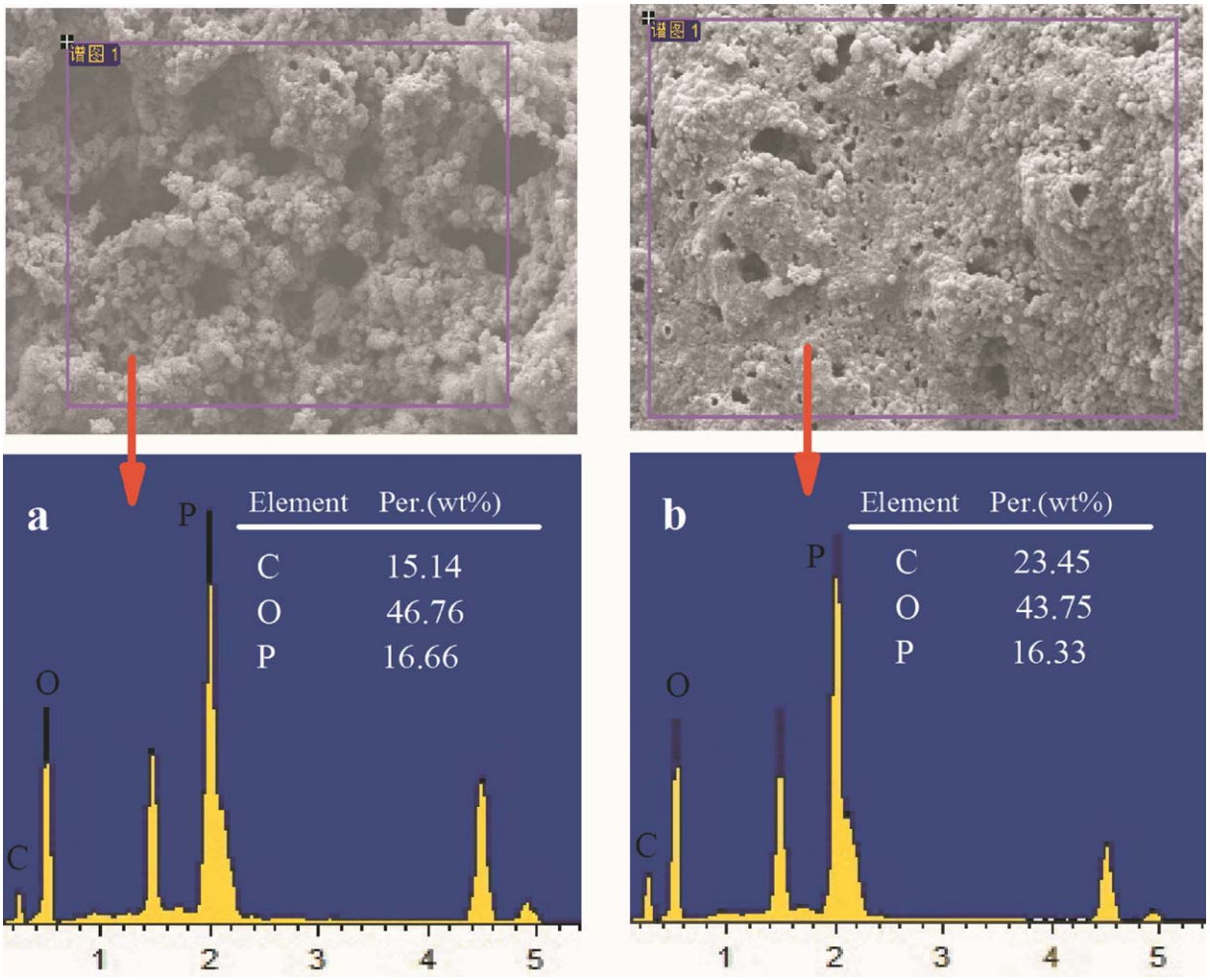

Figure 11. EDS spectra of the char residues after LOI testing: (a) LDPE/10MRP/20AHP and (b) LDPE/10MRP/30AHP. [Color figure can be viewed in the online issue, which is available at wileyonlinelibrary.com.]

To further investigate the flame-retardant mechanism, SEM–EDS was used to investigate the relationship between the microstructure of the chars and the flame retardancy of the LDPE/10MRP/AHP composites. As shown in Figure 9, the char residues of LDPE/10MRP were coarse and distributed in a disorderly manner, and it was easily damaged. Figure 10 shows the SEM micrographs of the char residue of the LDPE/10MRP/AHP composite after LOI testing. A lot of voids, such as craters, can be found in Figure 10(a); this was attributed to the spillage of gas produced by the composite when it decomposed. In addition, its surface was very coarse. Correspondingly, the char shown in Figure 10(d) was more compact with fewer voids; this indicated that the char layer of LDPE/10MRP/30AHP was more effective at slowing down heat and gas transference in the burning area. These results are consistent with those of the LOI and UL-94 tests.

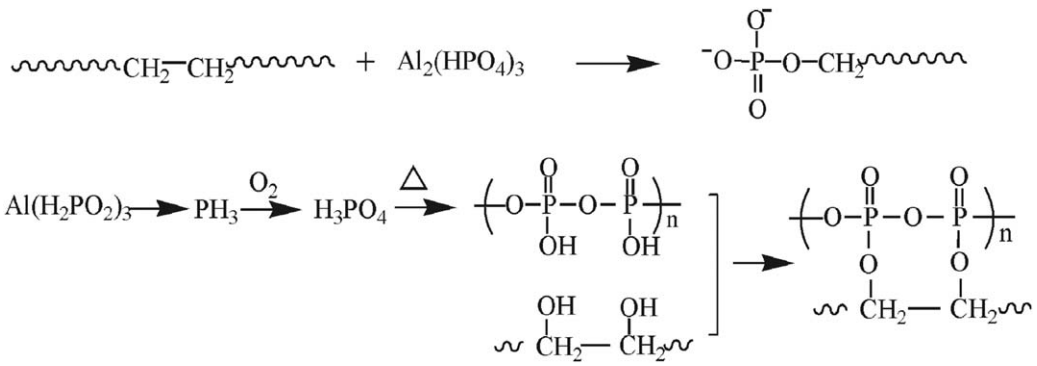

Figure 12. Schematic diagram of a possible way to generate a P—O—C bond.

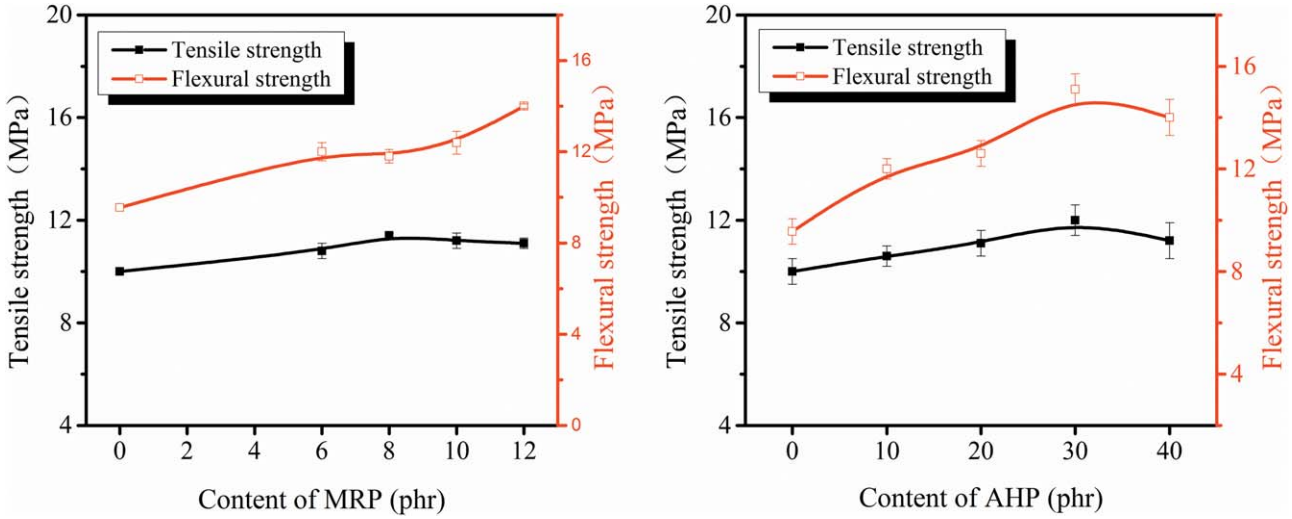

Figure 13. Effect of the flame-retardant content on the mechanical properties of the composites. [Color figure can be viewed in the online issue, which is available at wileyonlinelibrary.com.]

Moreover, these results were also proven by EDS testing. Figure 11 presents the EDS spectra of the LDPE/10MRP/AHP composite. We found that the intensity of the peak of carbon shown in Figure 11(b) was stronger than that shown in Figure 11(a). In addition, from the quantitative analysis of the elements, we observed that the char layer of the LDPE/10MRP/30AHP composite had a higher carbon content (23.45 wt %) than that of the LDPE/10MRP/20AHP composite (15.14 wt %). It is clear that a higher content of carbon can form a more compact char. On the other hand, this also showed that AHP promoted the formation of carbon.

According to FTIR spectroscopy and SEM–EDS analysis of the char, with increasing content of AHP, the char was more and more compact, and the content of carbon in the char was increasingly high. In addition, we also observed that the P—O—C bond was formed; this new bond could not only improve the thermostability of the char layer at high temperatures but could also promote char formation.[27] Therefore, the formation of the P—O—C bond was examined, and its possible generated mechanism was as follows. As illustrated in Figure 12, LDPE degraded in the way of random chain scission, and some hydroxyl groups were generated on the backbone after the dehydrogenation and oxidation of LDPE.[28,29] On the one hand, AHP could decompose into $Al_2(HPO_4)_3$ pyrophosphate.[30] These degradation products could react with the LDPE segment to generate P—O—C. On the other hand, AHP released phosphine, and then, part of the phosphine was quickly oxidized into phosphoric acid when the temperature increased. As the temperature increased further, phosphoric acid dehydrated and released water to form poly(phosphoric acid).[14] The hydroxyl groups on the backbone of the LDPE segment could react with poly(phosphoric acid) by dehydration.[29]

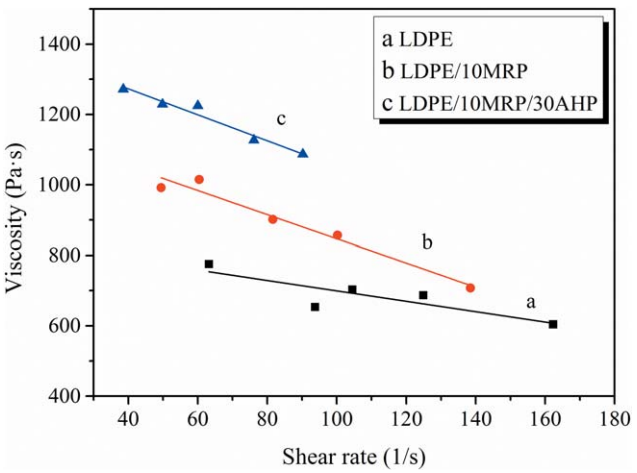

Figure 14. Effect of AHP and MRP on the rheological properties of LDPE. [Color figure can be viewed in the online issue, which is available at wileyonlinelibrary.com.]

Mechanical and Processing Properties

In addition to flame retardancy, the mechanical properties and processing properties were very important for flame-retardant LDPE. The effects of the flame retardants on the tensile strength and flexural strength of the flame-retardant LDPE are shown in Figure 13. As for the LDPE/MRP and LDPE/10MRP/AHP composites, the tensile strength had a similar tendency; this increased little in the observed concentration range. In other words, the addition of the flame retardant had little influence on the tensile strength of the composite. The flexural strength was improved after the addition of MRP and AHP, and the flexural strength increased to a maximum of 15.1 MPa, a rise of 57.9% in comparison with the value of 9.56 MPa of the LDPE composite. Figure 14 presents the effect of the flame retardants on the viscosity of the composites. We observed that the viscosities of LDPE/10MRP and LDPE/10MRP/30AHP were higher than that of the neat LDPE. The results suggest that the processing properties of the composite decreased with the addition of MRP or AHP.

Synergy between MRP and AHP

For MRP, at a high temperature, phosphorus oxides were generated when the MRP decomposed and then changed into

phosphoric acid, phosphorous acid, and so on through reaction with water. In addition, phosphoric acid became poly(phosphoric acid) via further dehydration. The poly(phosphoric acid) produced by MRP covered the surface of the composite and then suppressed the burning of the polymer. Meanwhile, AHP decomposed into $Al_2(HPO_4)_3$, $Al_4(P_2O_7)_3$, and PH_3; these degradation products reacted with the segment produced by the decomposition of LDPE. These reactions promoted the formation of the char and also improved the intensity of the char. The poly(phosphoric acid) produced by MRP and char were mixed, and this mixture covered the surface of the composite.[31] As a result, a protective barrier was formed; this barrier could be effective for significantly inhibiting the heat outside and the release of combustible gas. Consequently, the flame was inhibited, and the flame retardancy was remarkably improved. A kind of synergy took effect between MRP and AHP.

CONCLUSIONS

The stability of RP improved significantly after microencapsulation. Composites of LDPE with different contents of MRP or AHP were prepared and showed good performance in the burning of the composites. When the content of MRP was 10 phr and the content of AHP was 30 phr, the LOI value of the composite was 25.5%, and the UL-94 rating was V-0. The results of the cone calorimetry test revealed that AHP and MRP significantly decreased the peak heat release of the LDPE/AHP composites. The char residues increased with the incorporation of AHP in N_2, and the thermal stability improved at high temperatures. SEM–EDS verified that AHP promoted the formation of a compact char layer. AHP and MRP had a good synergistic effect and improved the barrier properties of the char layer; the polyphosphate produced by MRP and the char formed by AHP were mixed, and this mixture covered the surface of the composite. The P—O—Φ structure was generated and enhanced the intensity of the char.

REFERENCES

1. Chen, L.; Wang, Y. Z. *Polym. Adv. Technol.* **2010**, *21*, 1.
2. Xie, F.; Wang, Y. Z.; Yang, B.; Liu, Y. *Macromol. Mater. Eng.* **2006**, *291*, 247.
3. Sangcheol, K. J. *Polym. Sci. Part B: Polym. Phys.* **2003**, *41*, 936.
4. Cevdet, K.; Esin, I. J. *Fire Sci.* **2014**, *32*, 121.
5. Li, S. L.; Long, B. H.; Wang, Z. C.; Tian, Y. M.; Zheng, Y. H.; Zhang, Q. J. *Solid State Chem.* **2010**, *183*, 957.
6. Nihat, A. I.; Cevdet, K. J. *Fire Sci.* **2012**, *31*, 73.
7. Lomakin, S. M.; Dubnikova, I. L.; Shchegolikhin, A. N.; Zaikov, G. E.; Kozlowski, R.; Kim, G. M.; Michler, G. H. *J. Therm. Anal. Calorim.* **2008**, *94*, 719.
8. Cui, Z.; Qu, B. *J. Chin. J. Polym. Sci.* **2010**, *28*, 563.
9. Francis, R. C.; Udo, W.; Gert, H. *Polym. Degrad. Stab.* **2007**, *92*, 1813.
10. Yan, H. Y.; Wang, X.; Song, L.; Yu, B.; Yuan, Y.; Hu, Y.; Richard, K. K. Y. *Polym. Adv. Technol.* **2014**, *25*, 1034.
11. Zhao, B.; Hu, Y. *J. Appl. Polym. Sci.* **2011**, *119*, 2379.
12. Yang, W.; Song, L. *J. Appl. Polym. Sci.* **2011**, *122*, 1480.
13. Yang, W.; Hu, Y. *Compos. A* **2011**, *42*, 794.
14. Tang, G.; Wang, X.; Xing, W. Y.; Zhang, P.; Wang, B. B.; Hu, Y. *Ind. Eng. Chem. Res.* **2012**, *51*, 12009.
15. Li, Q. F.; Li, B.; Zhang, S. Q.; Lin, M. *J. Appl. Polym. Sci.* **2012**, *125*, 1782.
16. Cai, T. S.; Guo, F.; Chen, J. F. *Polym. Mater. Sci. Eng.* **2006**, *22*, 205.
17. Liu, J. C.; Yu, Z. L.; Chang, H. B.; Zhang, Y. B.; Shi, Y. Z.; Luo, J.; Pan, B. L.; Lu, C. *Polym. Degrad. Stab.* **2014**, *103*, 83.
18. Huang, X.; Qin, J.; Wan, D. J.; He, M.; Wu, D. K. *J. Guizhou Univ. Technol. Nat. Sci. Ed.* **2007**, *36*, 30.
19. Chang, H. C.; Lv, J. T.; Guo, Y. C.; Xu, Q. J. *China Plast. Ind.* **2011**, *39*, 89.
20. Li, J.; Liu, H. Y.; Wang, S. J.; You, L.; Wang, S. K. *CIESC J.* **2011**, *62*, 1716.
21. Wang, H. T.; Meng, X. F.; Wen, B.; Gao, X. W.; Zhang, S. M.; Yang, M. S. *Mater. Lett.* **2008**, *62*, 3745.
22. Antonietta, G.; Robert, A. S. *Compos. A* **2008**, *39*, 398.
23. Thomas, L. C.; Chittekden, R. A. *Spectrochim. Acta A* **1970**, *26*, 781.
24. Zhou, R. M.; Lai, X. J.; Li, H. Q.; Tang, S.; Zeng, X. R. *Polym. Compos.* **2014**, *35*, 158.
25. Chen, L. J.; Song, L.; Lv, P.; Jie, G. X.; Tai, Q. L.; Xing, W. Y. *Prog. Org. Coat.* **2011**, *70*, 59.
26. Zhu, S. W.; Shi, W. F. *Polym. Degrad. Stab.* **2003**, *80*, 217.
27. Yan, Y. W.; Huang, J. Q.; Guan, Y. H.; Shang, K.; Jian, R. K.; Wang, Y. Z. *Polym. Degrad. Stab.* **2014**, *99*, 35.
28. Gugumus, F. *Polym. Degrad. Stab.* **2002**, *77*, 147.
29. Feng, C. M.; Zhang, Y.; Lang, D. *Proc. Eng.* **2013**, *52*, 97.
30. Xiao, S. S.; Chen, M. J.; Dong, L. P. *Chin. J. Polym. Sci.* **2014**, *32*, 98.
31. Ballistreri, A.; Montaudo, G.; Puglisi, C.; Scamporrino, E.; Vitalini, D.; Calgari, S. J. *Polym. Sci. Polym. Chem. Ed.* **1983**, *21*, 679.